Farlow, JO, Falkingham, PL and Therrien, F

Pedal Proportions of Small and Large Hadrosaurs and Other Potentially Bipedal Ornithischian Dinosaurs

Pedal Proportions of Small and Large Hadrosaurs and Other Potentially Bipedal Ornithischian Dinosaurs

James O. Farlow [a], *, **Peter L. Falkingham** [b], and **François Therrien** [c]

*, [a] *corresponding author, Department of Biology, Purdue University Fort Wayne, 2101 East Coliseum Boulevard, Fort Wayne, IN 46805 USA; farlow@pfw.edu*

[b] *School of Biological and Environmental Sciences, Liverpool John Moores University, Liverpool, UK; p.l.falkingham@ljmu.ac.uk*

c *Royal Tyrrell Museum of Palaeontology, P.O. Box 7500, Drumheller, AB T0J 0Y0 Canada; Francois.Therrien@gov.ab.ca*

Highlights:

- **Foot skeletons of hadrosaurid dinosaurs show little shape change from small (young) to large (adult) individuals**
- **Foot skeletons of small (young) hadrosaurids are more similar in shape to those of large (adult) individuals than to those of small-bodied ornithischians of comparable size**
- **Small and large iguanodontian footprints of similar shape found in the same footprint assemblage could well have been made by conspecific dinosaurs**

Key words: Hadrosaurids; Ornithischia; Ichnology; Allometry

ABSTRACT: Foot skeletons of small (young) hadrosaurid dinosaurs were compared with those of large (adult) hadrosaurids to assess the extent of pedal shape change during ontogeny. Foot

skeletons of juvenile hadrosaurids were also compared with those of similar-sized adult, bipedal, non-hadrosaurian ornithischians to which the juvenile hadrosaurids were closer in size, to investigate the possibility that pedal shape change during hadrosaurid ontogeny would have been great enough for feet (and therefore footprints) of young hadrosaurids to have been more similar to those of small-bodied ornithischians than those of large adult hadrosaurids. Although possible allometric shape changes in hadrosaurid pedal proportions are detected, these are so subtle that the feet of young hadrosaurids are far more similar to those of adult hadrosaurs than those of small-bodied, non-hadrosaurid,ornithischians. Footprints made by conspecific hadrosaurids of different size and age are therefore likely to have been similar in shape, and footprints made by juvenile hadrosaurs are unlikely be misidentified as prints made by adults of smaller-bodied, more gracile, bipedal ornithischians.

1. Introduction

Because dinosaurs hatched from eggs, thereby limiting the maximum body size of a newly hatched individual, dinosaur species characterized by large adult body sizes could span a substantial ontogenetic size range (Carpenter, 1999). Footprints thought to have been made by small (or at least immature) dinosaurs are known for several trackmaker clades (Currie and Sarjeant, 1979; Lockley et al., 1994, 2006, 2012; Pascual-Arribas and Hernández-Medrano, 2011; Dalman, 2012; Kim et al., 2012, 2018, 2019; Fiorillo et al., 2014; Xing and Lockley, 2014; Fiorillo and Tykoski, 2016; Díaz-Martínez et al., 2015a; Castanera et al. 2020; Enriquez et al. 2021), but distinguishing footprints of a particular morphotype made by juveniles of large-bodied species from those of adults of small-bodied species remains challenging.

Hadrosaurids were large to enormous plant-eating dinosaurs that were prominent components of Late Cretaceous dinosaur faunas (Horner et al., 2004). Footprints made by large ornithopods, including hadrosaurids, are common in Cretaceous dinosaurian ichnofaunas (Lockley et al. 2014; Díaz-Martínez et al., 2015b). At some tracksites footprints attributed to hadrosaurids or other large iguanodontians come in distinct size classes, suggesting the possibility that they represent age-classes of a single species (Matsukawa et al., 1999, 2001; Fiorillo et al., 2014; cf. Lockley et al., 2012). This prompts questions of whether the feet (and thus footprints) of juvenile hadrosaurids can be expected to be similar in shape to those of larger individuals, only smaller, or whether they would also differ in shape from those of their elders, perhaps being closer in form to similar-sized feet of smaller-bodied adults of different ornithischian clades. As noted by Castanera et al. (2020: 408), "…little is known about the influence of ontogenetic changes in the feet of ornithopod dinosaurs and thus possible footprint shape variations." Might ontogenetic changes in hadrosaurid foot shape mirror phylogenetic changes observed from basal ornithopods through derived, large iguanodontians (Moreno et al. 2007)? In this study, we compare pedal dimensions in a large sample of hadrosaurids and bipedal, non-hadrosaurid ornithischians in order to assess ontogenetic change in pedal morphology among hadrosaurs, to determine if tracks left by juvenile hadrosaur feet could be confused with those left by adults of small-bodied ornithischians.

2. Materials and methods

2.1. Institutional abbreviations

CMNFV: Canadian Museum of Nature, Ottawa, Ontario; LACM: Natural History Museum of Los Angeles County, California; MOR: Museum of the Rockies, Bozeman, Montana; TMP: Royal Tyrrell Museum of Palaeontology, Drumheller, Alberta; YPM: Peabody Museum of Natural History, Yale University, New Haven, Connecticut.

2.2. Specimen descriptions

This study was specifically prompted by a report of juvenile individuals of *Prosaurolophus maximus* (Hadrosauridae, Saurolophinae) from the Upper Cretaceous Bearpaw Formation of southern Alberta (Drysdale et al., 2019)). In one of these specimens, TMP 2016.37.1 (Fig. 1A, B; supplemental animation [right]), between the left and right feet, metatarsals II and III and all the phalanges of the foot are preserved. A second specimen, TMP 1998.50.1, is less complete, but still preserves several pedal phalanges.

Prior to the description of these specimens, Prieto-Marquez and Guenther (2018) described perinatal specimens of *Maiasaura peeblesorum* (Hadrosauridae, Saurolophinae) from the Upper Cretaceous Two Medicine Formation of Montana. Among these was YPM VPPU 22400 (Fig. 1C; supplemental animation [left]), a composite right foot assembled from scattered bones of several young individuals of about the same size from the same locality (John R. Horner (personal communication 2 August 2018). This specimen is of particular interest due to its diminutive size (Wosik et al. 2017 described a very young *Edmontosaurus* individual of comparable size that regrettably did not preserve pedal phalanges), but its composite nature means it must be treated cautiously. Possible sources of error associated with treating the composite baby as a valid data point include both the possibility of misidentification of

phalanges and possible differences in relative proportions of phalanges among the different perinatal individuals.

A fourth small hadrosaurid specimen (MOR 471; Fig. 2D), identified as *Hypacrosaurus stebingeri* (Hadrosauridae, Lambeosaurinae), is intermediate in size between TMP 2016.37.1 and YPM VPPU 22400. We also measured a foot of *Edmontosaurus annectens* (Hadrosauridae, Saurolophinae; LACM 7233/23504) that is very close in size to TMP 2016.37.1.

2.3. Measurements and data analyses

We measured pedal phalanges of juvenile and adult hadrosaurids, and of other bipedal, or facultatively or potentially bipedal, ornithischians (Maidment and Barrett 2014). These include some basal ceratopsians (cf. Chinnery and Horner 2007; Senter 2007; Lee et al. 2011; Morschhauser et al. 2018; Slowiak et al. 2019). We did not, however, include stegosaurs, which some authors (e.g. Gierliñski and Sabath 2008) have interpreted as bipedal, but which most workers regard as quadrupedal (Maidment and Barrett 2014).

Measurements were made by ourselves (mostly by Farlow) on the phalanges of digits II-IV of the ornithischians examined in this study. The innermost hindfoot toe (digit I) is present in basal ornithopods and in ceratopsians, but is lost in derived iguanodontians, including hadrosaurids (Moreno et al. 2007), and so will not be considered in this study (but see Farlow et al. 2018 for a consideration of the relative size of digit I in bipedal dinosaurs more generally).

Phalanges were measured following the protocols of Farlow et al. (2018: pp. 10-11; Fig. 2 here). Non-ungual phalanx lengths were measured on the medial and lateral sides of the bone, from roughly the dorsoventral midpoint along the concave proximal articular end to roughly the

dorsoventral midpoint along the convex distal articular end of the bone. Ungual lengths were measured in a straight-line manner on the medial and lateral sides of the bone from roughly the dorsoventral midpoint along the concave proximal articular end of the bone to the tip of the bone. For specimens in which only the medial or lateral length could be measured, that value was used in the analysis; otherwise the medial and lateral lengths were averaged. Widths were the maximum transverse dimension along the distal ends of non-ungual phalanges.

The specific measurements used in this study were those that could readily be made on TMP 2016.37.1. Measurements for that specimen, TMP 1998.50.1, MOR 471, and YPM VPPU 22400 are given in Table 1; measurements for other ornithischian feet are taken from Farlow et al. (2018: Appendix Table A1.1, pp. 379-391), which provides detailed information about the specimens.

Both bivariate and multivariate analyses of measurements were done, using IBM SPSS Statistics version 26. For investigations of allometry and for principal components analysis (PCA), the parameters compared were log-transformed prior to analysis. For investigations of allometry, both ordinary least squares (OLS) regression and reduced major axis (RMA) bivariate analyses were done, both including and excluding the composite neonate specimen of *Maiasaura*. Allometry was inferred if the 95 % confidence interval (CI) of the slope of the bivariate analysis excluded a value of 1.000. For RMA analyses, the CIs were mostly calculated in SPSS following Rayner (1985: Table 1) and Leduc (1987), but for CIs that this protocol that presented as statistically significant, the CIs were also calculated in the statistical package Past version 4.06 (cf. Hammer et al., 2001). Due to the relatively small sample size of measurable foot skeletons, each foot was treated as an independent data case, and no attempt was made to consider the effects of different numbers of specimens across taxa, or to correct for variable

phylogenetic propinquity. However, we do note where a particular taxon may be strongly affecting the overall results.

3. Results

3.1. Principal components analysis

In the PCA of the entire ornithischian sample, including the composite baby *Maiasaura* specimen (Table 2), more than 90 % of the data variance is associated with the first principal component. All of the pedal parameters show positive loadings on that first component, indicating that it is associated with overall size. The remaining data variance is mainly associated with PC 2 (about 5 %) and PC 3 (about 1.5 %).

Variables with positive loadings on PC 2 are the lengths of phalanges distal to the first (most proximal) phalanx of digits II-IV, while variables with negative loadings are the lengths of the first (most proximal) phalanges of the three digits and the widths of phalanges III2 and IV2. Hadrosaurids and other large iguanodontians plot more negatively along PC 2 than other ornithischians in the sample (Fig. 3A), with the single data case for *Camptosaurus* plotting between the trends for the relatively stout hadrosaurids and other large iguanodontians, on the one hand, and the more gracile ornithischians on the other (cf. Gierliński and Sabath 2008). Hadrosaurids and large iguanodontians, and the more gracile ornithischians, show parallel trends along PC 2, with hadrosaurids and other big iguanodontians becoming less negative, and the gracile forms increasingly positive, with increasing foot size. The small, juvenile hadrosaurids plot along the overall large-ornithopod trend of PC 2, much more negatively than gracile ornithischians of comparable size.

Scatterplots of selected aspects of PC 2 (Fig. 3B, C) allow exploration of these shape features with more data cases than PC 2 itself, because they allow use of data cases for which some of the components of PC 2 could not be measured. Plotting the ratio of the combined length of phalanges III2-III4 to the length of phalanx III1 (Fig. 3B) again shows the larger iguanodontians to have relatively shorter distal phalanges than more gracile ornithischians, with *Tenontosaurus* in the gracile group displaying an interesting tendency to increase the relative length of the distal part of the toe with increasing digit III length. The smaller hadrosaurids are clearly more like their larger kin than like gracile ornithischians of similar size in this comparison; hadrosaurids show no strong tendency for size-related change (but see below) in the ratio, especially if the *Maiasaura* baby is included in the sample (although *Edmontosaurus*, one of the biggest hadrosaurids in the sample, seems to take larger values of the ratio than other, smaller hadrosaurids).

The relative width of phalanx III2 (Fig. 3C) is another aspect of PC 2. Across the ornithischians in our sample, the relative breadth of phalanx III2 increases with increasing animal size (cf. Moreno et al. 2007; Lockley 2009; Farlow et al. 2018). However, the smaller, younger hadrosaurid specimens again are more like their elders than like gracile ornithischians to which they are more similar in size. There is no indication of an increase in relative stoutness of digit III with increasing digit length in hadrosaurids.

Variables with positive loadings on PC 3 (Table 2) include the lengths of all the non-ungual phalanges of digits II-IV, while variables with negative loadings include the ungual lengths, and to a lesser extent phalanx widths. A scatterplot of PC 3 against PC 1 (Fig. 3D) doesn't provide as clear separation of hadrosaurids from gracile ornithischians, but it does distinguish hadrosaurids from other large iguanodontians, with hadrosaurids taking more positive

values of PC 3. There is a suggestion that PC 3 may become more positive with increasing size in hadrosaurids, if the composite *Maiasaura* baby is included in the sample.

The ratio of ungual III4 length to the combined lengths of non-ungual phalanges of digit III (Fig. 3E) is an aspect of PC 3, with higher values of the ratio associated with more negative values of PC 3. The relative length of ungual III4 of hadrosaurids is comparable to that of many gracile ornithischians, although *Tenontosaurus* has a relatively longer ungual that becomes proportionally even longer with increasing size. Hadrosaurids have a relatively shorter ungual than other big iguanodontians. Because more positive values of PC3 are associated with relatively long non-ungual phalanges (Table 2), and, as already noted, hadrosaurids may show more positive values of PC3 with increasing foot size (Fig. 3D), one might expect ungual III4 to become shorter with respect to the length of the non-ungual phalanges of digit III with increasing size, but this does not occur (Fig. 3E). If anything, ungual III4 becomes relatively longer, especially in *Edmontosaurus*.

3.2. Bivariate comparisons in hadrosaurids

Restricting comparisons to hadrosaurs, and to comparisons of relative sizes of phalangeal parameters within single digits, allows further exploration of the trends identified by PCA with a larger sample size. Consistent with the relationship between PC 2 and PC 1 seen in hadrosaurids (Fig. 3A), the slope of the log-transformed length of phalanx III2 against that of phalanx III1 in hadrosaurids is greater than 1, whether the composite *Maiasaura* baby is included or not in the sample, and whether the slope is computed with an OLS regression or reduced major axis model (Table 3). However, the 95 % confidence interval of the slope does not exclude a value of 1 in

any of the four versions of the relationship, and so the slopes are not significantly different than 1 (isometry). The relationship between the log-transformed length of phalanx III3 against that of phalanx III1, in contrast, has calculated slope values less than 1 in three of the four versions of the relationship, but again without any of the 95 % confidence limits excluding 1. The slope of the log-transformed combined lengths of phalanges III2-III4 against the log-transformed length of phalanx III1 in the four versions of the relationship shows the same pattern of results as seen in the four versions of the relationship between the log-transformed length of phalanx III2 against the log-transformed phalanx III1 (Fig. 3B). All told, these results suggest, but do not demonstrate, the possibility of positive allometry of the length of at least some of the more distal phalanges relative to the length of the first phalanx of digit III. For digit II, in contrast to digit III, the relationship between the log-transformed combined lengths of the distal phalanges against the log-transformed length of the first phalanx (Table 3) does not show consistent patterns across the four versions of the relationship. For digit IV three of the four versions of the relationship between log-transformed combined lengths of the distal phalanges against the log-transformed length of the first phalanx have slopes less than 1. For none of the relationships between proximal and distal phalanges in digits II and IV does the slope differ significantly from 1.

The relative widths of phalanges have negative loadings on both PC 2 and PC 3 (Table 2). Three of the four versions of the relationship between log-transformed phalanx III2 width and log-transformed digit III length have slopes greater than 1 (Table 3), but in none of these does the slope differ significantly from 1 (cf. Fig. 3C).

The lengths of the unguals relative to the lengths of non-ungual phalanges are the main contributors to PC 3 (Fig. 3D, 3E). For digit III, the relationship between log-transformed ungual length and the log-transformed combined lengths of the non-ungual phalanges has slopes with

values greater than 1 in all four versions of the comparison (Table 3); if the composite baby *Maiasaura* foot is excluded from the comparison, both the regression and the RMA slopes have 95 % confidence limits whose minimum values are at least barely greater than 1. For digit II, three of the four versions of the corresponding comparison yield slopes greater than 1, albeit without being significantly different than 1. For digit IV, in contrast, the slopes of all four versions of the relationship are less than 1, but again without being significantly different than 1.

Across the ornithischians in our sample, two clear tendencies are observed as animal size increases: 1) an increase in aggregate length of the phalanges of digit II (Fig. 4A), but not digit IV (Fig. 4B), relative to the aggregate length of the phalanges of digit III; and 2) decrease in length of digit IV relative to the length of digit II (Fig. 4C). Hadrosaurids do not differ from other ornithischians of comparable size in the relative lengths of the three digits.

For hadrosaurids alone, if the composite *Maiasaura* baby is included in the sample, OLS regression and RMA slopes, for both log-transformed digits II and IV, show slight but significant positive allometry with respect to the length of log-transformed digit III, and also with respect to the log-transformed length of just phalanx III1 (probably the most important weight-bearing bone of the digital portion of the foot) (Table 3). Excluding the composite *Maiasaura* baby, the RMA slopes for the log-transformed lengths of both digits II and IV, against the log-transformed length of digit III, remain at least slightly greater than 1 without being statistically significant. Excluding the composite *Maiasaura* baby, the regression slope for log-transformed digit IV against the log-transformed length of digit III is also greater than 1, but that of log-transformed digit II is less than 1, with neither of these slopes being statistically significant. Again excluding the composite *Maiasaura* baby, both regression and RMA slopes of the relationship between log-transformed digit II and IV length and log-transformed phalanx III1 length are greater than 1,

with the RMA slope between log-transformed digit IV length and log III1 length being slightly but significantly greater than 1. The RMA and regression slopes of log-transformed digit IV length against the log-transformed length of digit II are greater than 1, albeit just barely if the composite *Maiasaura* baby is excluded, but none of these slopes is significantly different than 1.

4. Concluding Remarks

Although, as usual in dinosaur paleontology, additional specimens, particularly of very young hadrosaurids, would be desirable, some conclusions about ontogeny and foot shape seem valid. Across the size range of hadrosaurids in our sample, there are suggestions of at least subtle shape change from small to large individuals, but most of these are not statistically significant. Those that are significant are greatly affected by whether or not the composite *Maiasaura* baby, whose foot is much smaller than that of any other pedal specimen in our sample, is included in the analysis.

Even if the composite *Maiasaura* baby foot is included in the comparison, it appears that very young hadrosaurids had feet more similar in shape to those of their large elders than to feet of similar-sized, non-hadrosaurid ornithischians (Figs. 1, 3, 4). Any allometric changes in foot, and thus footprint, shape during ontogeny would not have been great enough for the juvenile pes or pes print to look recognizably different from that of an adult in any feature other than size (cf. Dodson 1986 for ceratopsids). Stating things baldly—and perhaps with a degree of exaggeration--over the span of its lifetime, a hadrosaurid (and presumably any other large-bodied iguanodontian as well) would likely not have transitioned from making *Anomoepus*-like

267 footprints as a neonate to making *Caririchnium*-like or *Hadrosauropodus*-like footprints as a
268 fully-grown adult.

269 This conclusion corroborates inferences from the ichnological record. Published
270 descriptions of footprints attributed to large iguanodontians commonly report two size
271 parameters, footprint length and width. Footprints assigned to the (possibly questionable:
272 Lockley et al., 2014; Díaz-Martínez et al., 2015b) ichnogenus *Ornithopodichnus* from the Lower
273 Cretaceous of Korea and China (Kim et al., 2009; Lockley et al., 2012; Xing and Lockley, 2014)
274 span a significant size range, with lengths ranging ca. 12-43 cm. (Interestingly, the smaller
275 footprints would have been made by dinosaurs about the same size as our TMP 2016.37.1.) The
276 length: width ratio of the small and large prints is very similar, suggesting relatively little or no
277 shape change between the small and large trackmakers (as noted by Lockley et al. 2012). The
278 same is true of *Caririchnium* from the mid-Cretaceous Dakota Group of Colorado (Matsukawa et
279 al., 1999), *Hadrosauropodus* from the Upper Cretaceous Cantwell Formation of Alaska (Fiorillo
280 et al., 2014; Fiorillo and Tykoski, 2016), and *Amblydactylus* (or *Caririchnium*—Díaz-Martínez
281 et al., 2015b) from the Lower Cretaceous Gething Formation (Fig. 5) of British Columbia
282 (Currie and Sarjeant, 1979). The lack of dramatic pedal shape change between small and large
283 hadrosaurids reported in this study suggests—but obviously does not prove, given the likely
284 similarity of foot shape across large iguanodontian trackmaker species—that small and large
285 specimens of iguanodontian footprints of similar shape, found at the same tracksite or at least in
286 the same ichnofauna, could well have been made by juvenile and adult individuals of the same
287 zoological species.

288

289 **5. Acknowledgments**

We thank Dan Brinkman for facilitating access to the composite *Maiasaura* baby foot, and Jack Horner for information about its composition. Jens Lallensack provided useful discussion; Peter Dodson and Martin Lockley provided helpful reviews that greatly improved our text and analyses. Jim Whitcraft assisted in the production of figures. This research was supported by NSF EAR 9612880 to Farlow.

6. References

Carpenter, K. 1999. Eggs, Nests, and Baby Dinosaurs. Indiana University Press, Bloomington, Indiana.

Castanera, D., Silva, B.C., Santos, V.F., Malafaia, E., and Belvedere, M. 2020. Tracking Late Jurassic ornithopods in the Lusitanian Basin of Portugal: ichnotaxonomic implications. Acta Palaeontologica Polonica 65, 399-412.

Chinnery, B.J., and Horner, J.R. 2007. A new neoceratopsian dinosaur linking North American and Asian taxa. Journal of Vertebrate Paleontology 27, 625-641.

Currie, P.J., and Sarjeant, W.A.S. 1979. Lower Cretaceous dinosaur footprints from the Peace River Canyon, British Columbia, Canada. Palaeogeography, Palaeoclimatology, Palaeoecology 28, 103-115.

Dalman, S.G., 2012. New data on small theropod footprints from the Early Jurassic (Hettangian) Hartford Basin of Massachusetts, United States. Bulletin of the Peabody Museum of Natural History 53, 333-353.

Díaz-Martínez, I., García-Ortiz, E., and Pérez-Lorente, F., 2015a. A new dinosaur tracksite with small footprints in the Urbión Group (Cameros Basin), Lower Cretaceous, La Rioja, Spain). Journal of Iberian Geology 41, 167-175.

Díaz-Martínez, I., Pereda-Suberbiola, X., Pérez-Lorente, F., and Canudo, J.I., 2015b. Ichnotaxonomic review of large ornithopod dinosaur tracks: temporal and geographic implications. PLoS One 10(2):e115477.doi:10.1371/journal.pone.0115477.

Dodson, P. 1986. *Avaceratops lammersi*: a new ceratopsid from the Judith River Formation of Montana. Proceedings of the Academy of Natural Sciences of Philadelphia 138: 305-317.

Drysdale, E.T., Therrien, F., Zelenitsky, D.K., Weishampel, D.B., and Evans, D.C., 2019. Description of juvenile specimens of *Prosaurolophus maximus* (Hadrosauridae, Saurolophinae) from the Upper Cretaceous Bearpaw Formation of southern Alberta, Canada, reveals ontogenetic changes in crest morphology. Journal of Vertebrate Paleontology. DOI: 10.1080/02724634.2018.1547310.

Enriquez, N.J., N.E. Campione, T. Brougham, F. Fanti, M.A. White, R.L. Sissons, C. Sullivan, M.J. Vavrek, and P.R. Bell. 2021. Exploring possible ontogenetic trajectories in tyrannosaurids using tracks from the Wapiti Formation (Upper Campanian) of Alberta, Canada. Journal of Vertebrate Paleontology, DOI: 10.1080/02724634.2021.1878201.

Farlow, J.O., Coroian, D., and Currie, P.J. 2018. Noah's Ravens: Interpreting the Makers of Tridactyl Dinosaur Footprints. Indiana University Press, Bloomington, Indiana.

Fiorillo, A.R., and Tykoski, R.S. 2016. Small hadrosur manus and pes tracks from the lower Cantwell Formation (Upper Cretaceous) Denali National Park, Alaska: implications for locomotion in juvenile hadrosaurs. Palaios 31, 479-482.

Fiorillo, A.R., Hasiotis, S.T., and Kobayashi, Y. 2014. Herd structure in Late Cretaceous polar dinosaurs: a remarkable new dinosaur tracksite, Denali National Park, Alaska, USA. Geology 42, 719-722.

Gierliński, G., and K. Sabath. 2008. Stegosaurian footprints from the Morrison Formation of Utah and their implications for interpreting other ornithischian tracks. Ocrytos 8, 29-46.

Hammer, Ø., Harper, D.A.T., and Ryan, P.D. 2001. Past: Palaeontological statistics software package for education and data analysis. Palaeontologia Electronica 4; http://palaeo-electronica.org/2001_past/issue1_01.html.

Horner, J.R., Weishampel, D.B., and Forster, C.A., 2004. Hadrosauridae. In: Weishampel, D.B., Dodson, P., & Osmólska, H. (Eds.), The Dinosauria. Second Edition. University of California Press, Berkeley, 438-463.

Kim, K.S., Lockley, M.G., Kim, Y.K., and Seo, S.J., 2012. The smallest dinosaur tracks in the world: occurrences and significance of *Minisauripus* from east Asia. Ichnos 19, 66-74.

Kim, K.S., Lim, J.D., Lockley, M.G., Xing, L., Kim, D.H., Piñuela, L., Romilio, A., Yoo, J.S., and Ahn, J., 2018: Smallest known raptor tracks suggest microraptorine activity in lakeshore setting. Scientific Reports 8:16908/doi:10.1038/s41598-018-35289-4.

Kim, K.S., Lockley, M.G., Lim, J.D., and Xing, L., 2019. Exquisitely-preserved, high-definition skin traces in diminutive theropod tracks from the Cretaceous of Korea. Scientific Reports 9: 2039/https://doi.org/10.1038/s41598-019-38633-4.

Kim, J.Y., Lockley, M.G., Kim, H.M., Lim, J.-D., and Kim, K.S. 2009. New dinosaur tracks from Korea, *Ornithopodichnus masanensis* ichnogen. et ichnosp. nov. (Jindong

Formation, Lower Cretaceous): implications for polarities in ornithopod foot morphology. Cretaceous Research 30, 1387-1397.

Leduc, D.J. 1987. A comparative analysis of the reduced major axis technique of fitting lines to bivariate data. Canadian Journal of Forestry Research 17, 654-659.

Lee, Y.-N., Ryan, M.J., and Kobayashi, Y. 2011. The first ceratopsian dinosaur from Korea. Naturwissenschaften 98, 39-49.

Lockley, M.G. 2009. New perspectives on morphological variation in tridactyl footprints: clues to widespread convergence in developmental dynamics. Geological Quarterly 53, 415-432.

Lockley, M.G., Huh, M., and Kim, B.S. 2012.*Ornithopodichnus* and pes-only sauropod trackways from the Hwasun tracksite, Cretaceous of Korea. Ichnos 19, 93-100.

Lockley, M.G., Meyer, C.A., and dos Santos, V.F., 1994. Trackway evidence for a herd of juvenile sauropods from the Late Jurassic of Portugal. Gaia 10, 27-35.

Lockley, M.G., Xing, L., Lockwood, J.A.F., and Pond, S. 2014. A review of large Cretaceous ornithopod tracks, with special reference to their ichnotaxonomy. Biological Journal of the Linnean Society 113, 721-736.

Lockley, M.G., Houck, K., Yang, S.-Y., Matsukawa, M., and Kim, S.-K., 2006. Dinosaur-dominated footprint assemblages from the Cretaceous Jindong Formation, Hallyo Haesang National Park area, Goseong County, South Korea: evidence and implications. Cretaceous Research 27, 70-101.

Maidment, S. C. R., and Barrett, P. M. 2014. Osteological correlates for quadrupedality in ornithischian dinosaurs. Acta Palaeontologica Polonica 59, 53-70.

Matsukawa, M., Lockley, M.G., and Hunt, A.P., 1999. Three age groups of ornithopods inferred from footprints in the mid-Cretaceous Dakota Group, eastern Colorado, North America. Palaeogeography, Palaeoclimatology, Palaeoecology 147, 39-51.

Matsukawa, M., Matsui, M., and Lockley, M.G., 2001. Trackway evidence of herd structure among ornithopod dinosaurs from the Cretaceous Dakota Group of northeastern New Mexico, USA. Ichnos 8, 197-206.

Moreno, K., M.T. Carrano, and K. Snyder. 2007. Morphological changes in pedal phalanges through ornithopod dinosaur evolution: a biomechanical approach. Journal of Morphology 268, 50-63.

Morschhauser, E. M., You, H., Li, D., and Dodson, P. 2018. Postcranial morphology of the basal neoceratopsian (Ornithischia: Ceratopsia) *Auroraceratops rugosus* from the Early Cretaceous (Aptian-Albian) of northwestern Gansu Province, China. Journal of Vertebrate Paleontology Memoir 18, Volume 38 Supplement, 75-116.

Pascual-Arribas, C., and Hernández-Medrano, N., 2011. Posibles huellas de crías de terópodo en el Yacimiento de Valdehijuelos (Soria, España). Studia Geologica Salmanticensia 47, 77-110.

Prieto-Marquez, A., and Guenther, A.F., 2018. Perinatal specimens of *Maiasaura* from the Upper Cretaceous of Montana (USA): insights into the early ontogeny of saurolophine hadrosaurid dinosaurs. PeerJ 6:e4734; DOI 10.7717/peerj.4734.

Rayner, J.M.V. 1985. Linear relations in biomechanics: the statistics of scaling functions. Journal of Zoology, London 206, 415-439.

Senter, P. 2007. Analysis of forelimb function in basal ceratopsians. Journal of Zoology 273, 305-314.

Slowiak, J., Tereshchenko, V.S., and Fostowicz-Frelik, L. 2019. Appendicular skeleton of *Protoceratops andrewsi* (Dinosauria, Ornithischia): comparative morphology, ontogenetic changes, and the implications for non-ceratopsid ceratopsian locomotion. PeerJ 7: e7324 DOI 10.7717/peerj.7324.

Wosik, M., M.B. Goodwin, and D.C. Evans. 2017. A nestling-sized skeleton of *Edmontosaurus* (Ornithischia, Hadrosauridae) from the Hell Creek Formation of northeastern Montana, U.S.A., with an analysis of ontogenetic limb allometry. Journal of Vertebrate Paleontology 37, DOI: 10.1080/02724634.2017.1398168.

Xing, L., and Lockley, M.G. 2014. First report of small *Ornithopodichnus* trackways from the Lower Cretaceous of Sichuan, China. Ichnos 21, 213-222.

Table 1. Measurements of pedal phalanges of juvenile hadrosaurids; measurements used are those parameters measurable on TMP 2016.37.1 (Fig. 1A, B). All measurements in millimeters.

Species	Specimen	Phalanx Length (L) or Distal Width (dw)					
Prosaurolophus maximus	TMP 2016.37.1	II1L: 78	II2L: 31	II3L: 47			
		III1L: 73	III2L: 23	III2dw: 71	III3L: 18	III4L: 46	
		IV1L: 57	IV2L: 12	IV2dw: 51	IV3L: 11	IV4L: 15	IV5L: 45
Prosaurolophus maximus	TMP 1998.50.1	II1L: 67	II2L: 21	II3L: 39			
		III1L: 62	III2L:				
		IV1L: 53	IV2L: 15		IV3L: 8		IV5L: 32
Hypacrosaurus stebingeri	MOR 471 TM-019	II1L: 64	II2L: 21	II3L: 41			
		III1L: 65	III2L: 17	III2dw: 54	III3L: 13	III4L: 39	
		IV1L: 46	IV2L: 12	IV2dw: 39	IV3L: 9	IV4L: 9	IV5L: 40
Maiasaura peeblesorum composite foot	YPM VPPU 22400	II1L: 14	II2L: 7	II3L: 11			
		III1L: 19	III2L: 6	III2dw: 15	III3L: 6	III4L: 14	
		IV1L: 11	IV2L: 4	IV2dw: 9	IV3L: 3	IV4L: 3	IV5L: 11

408

409

Table 2. Principal components analysis (PCA, using a covariance matrix) of log-transformed linear dimensions of pedal phalanges of bipedal and potentially bipedal ornithischian dinosaurs. Parameters used in the analysis are those that could be measured in TMP 2016.37.1. Number of specimens = 36.

Parameter	PC1 loading (raw [rescaled])	PC2 loading (raw [rescaled])	PC3 loading (raw [rescaled])
Phalanx II1 Length	0.281 (0.979)	-0.043 (-0.148)	0.023 (0.079)
Phalanx II2 Length	0.224 (0.974)	0.016 (0.069)	0.039 (0.169)
Phalanx (Ungual) II3 Length	0.250 (0.952)	0.042 (0.161)	-0.061 (-0.234)
Phalanx III1 Length	0.279 (0.960)	-0.075 (-0.257)	0.024 (0.082)
Phalanx III2 Length	0.200 (0.937)	0.048 (0.223)	0.047 (0.222)
Phalanx III2 Distal Width	0.336 (0.959)	-0.093 (-0.266)	-0.009 (-0.027)
Phalanx III3 Length	0.184 (0.924)	0.063 (0.314)	0.026 (0.132)
Phalanx (Ungual) III4 Length	0.244 (0.957)	0.047 (0.184)	-0.047 (-0.185)
Phalanx IV1 Length	0.292 (0.975)	-0.056 (-0.186)	0.022 (0.074)
Phalanx IV2 Length	0.210 (0.913)	0.085 (0.368)	0.017 (0.073)
Phalanx IV2 Distal Width	0.338 (0.978)	-0.062 (-0.178)	-0.023 (-0.066)
Phalanx IV3 Length	0.197 (0.912)	0.082 (0.381)	0.012 (0.055)
Phalanx IV4 Length	0.202 (0.922)	0.072 (0.328)	0.009 (0.043)
Phalanx (Ungual) IV5 Length	0.265 (0.977)	0.023 (0.084)	-0.048 (-0.176)
Eigenvalues (&% of variance)	0.910 (91.662)	0.053 (5.348)	0.015 (1.552)
Cumulative variance explained (%)	91.662	97.010	98.562
Kaiser-Meyer-Olkin Measure of Sampling Adequacy = 0.927; Bartlett's Test of Sphericity: chi-square = 1366.093, $p < 0.001$			

Table 3. Regression and reduced major axis slopes of bivariate relationships between log-transformed linear measurements of hadrosaur foot skeletons. "Including" and "excluding" refer to whether or not the composite foot skeleton of the neonate *Maiasaura peeblesorum* specimen is included in the sample. Slope values in **bold** have a 95 % CI that excludes 1.000, indicating that the slope has a value significantly different than 1. For RMA slopes that present as statistically different than 1, the 95 % CI was calculated two ways: following Rayner (1985) and Leduc (1987) (top line), and using the program PAST (Hammer et al., 2001; bottom line).

Independent Variable	Dependent Variable	Method	Sample	R^2	Slope	95 % CI	N
Phalanx III1 Length	Phalanx III2 Length	Regression	Including	0.885	1.063	0.905-1.221	27
			Excluding	0.667	1.072	0.753-1.390	26
		RMA	Including	0.885	1.130	0.973-1.312	27
			Excluding	0.667	1.312	0.965-1.783	26
	Phalanx III3 Length	Regression	Including	0.822	0.895	0.723-1.067	27
			Excluding	0.590	0.980	0.636-1.324	26
		RMA	Including	0.822	0.988	0.813-1.199	27
			Excluding	0.590	1.276	0.884-1.841	26
	Combined Length Phalanges III2-III4	Regression	Including	0.912	1.012	0.873-1.151	24
			Excluding	0.754	1.099	0.814-1.384	23
		RMA	Including	0.912	1.060	0.923-1.217	24
			Excluding	0.754	1.265	0.971-1.650	23
Digit III Length Excluding Ungual	Digit III Ungual Length	Regression	Including	0.952	1.058	0.953-1.163	24
			Excluding	0.884	**1.198**	1.002-1.395	23
		RMA	Including	0.952	1.085	0.982-1.198	24
			Excluding	0.884	**1.274**	1.079-1.504	23

						1.049-1.399	
Phalanx II1 Length	Combined Length Phalanges II2-II3	Regression	Including	0.955	0.974	0.878-1.070	23
			Excluding	0.878	1.060	0.876-1.245	22
		RMA	Including	0.955	0.997	0.903-1.100	23
			Excluding	0.878	1.132	0.950-1.349	22
Digit II Length Excluding Ungual	Digit II Ungual Length	Regression	Including	0.933	0.991	0.871-1.111	23
			Excluding	0.814	1.027	0.798-1.256	22
		RMA	Including	0.933	1.026	0.908-1.159	23
			Excluding	0.814	1.138	0.907-1.428	22
Phalanx IV1 Length	Combined Length Phalanges IV2-IV5	Regression	Including	0.947	0.945	0.837-1.052	21
			Excluding	0.829	0.989	0.767-1.212	20
		RMA	Including	0.947	0.971	0.866-1.088	21
			Excluding	0.829	1.086	0.864-1.366	20
Digit IV Length Excluding Ungual	Digit IV Ungual Length	Regression	Including	0.941	0.942	0.829-1.055	21
			Excluding	0.803	0.882	0.686-1.098	20
		RMA	Including	0.941	0.971	0.860-1.096	21
			Excluding	0.803	0.984	0.766-1.264	20
Digit III Length	Digit II Length	Regression	Including	0.986	**1.100**	1.036-1.164	20
			Excluding	0.959	0.992	0.888-1.096	19
		RMA	Including	0.986	**1.108**	1.044-1.175	20
						1.073-1.254	
			Excluding	0.959	1.013	0.911-1.126	19
	Digit IV Length	Regression	Including	0.987	**1.106**	1.043-1.169	20
			Excluding	0.954	1.059	0.940-1.178	19
		RMA	Including	0.987	**1.113**	1.051-1.178	20
						1.072-1.223	
			Excluding	0.954	1.084	0.968-1.213	19

Phalanx III1 Length	Digit II Length	Regression	Including	0.981	**1.116**	1.042-1.189	21
			Excluding	0.939	1.080	0.943-1.216	20
		RMA	Including	0.981	**1.126**	1.053-1.204	21
						1.057-1.205	
			Excluding	0.939	1.114	0.981-1.264	20
	Digit IV Length	Regression	Including	0.974	**1.117**	1.030-1.204	21
			Excluding	0.907	1.128	0.949-1.306	20
		RMA	Including	0.974	**1.132**	1.046-1.224	21
						0.982-1.200	
			Excluding	0.907	**1.184**	1.009-1.389	20
						1.047-1.342	
Digit II Length	Digit IV Length	Regression	Including	0.991	1.002	0.949-1.055	17
			Excluding	0.968	1.057	0.947-1.167	16
		RMA	Including	0.991	1.007	0.955-1.061	17
			Excluding	0.968	1.074	0.967-1.193	16
Digit III Length	Phalanx III2 Distal Width	Regression	Including	0.960	1.018	0.921-1.114	22
			Excluding	0.858	0.941	0.758-1.125	21
		RMA	Including	0.960	1.039	0.944-1.143	22
			Excluding	0.858	1.016	0.833-1.238	21

412

413

414

Fig. 1. Foot skeletons of small and large specimens of hadrosaurs. Scale bar in panels A-D = 5 cm. (A, B) Nearly complete left pedal skeleton of TMP 2016.37.1, *Prosaurolophus maximus*. As preserved, digit II is folded beneath digits III and IV. Individual phalanges are labeled. (A) Dorsal view, showing digits III and IV. The ungual of digit III is missing on this foot, but preserved in the right foot. (B) Ventral view, showing digit II. (C) Dorsal view of composite right foot skeleton of YPM VPPU 22400, *Maiasaura peeblesorum*. (D) Dorsal view of right foot skeleton of MOR 471, *Hypacrosaurus stebingeri*. (E) Anterior oblique view right foot of CMNFV 8501, *Hypacrosaurus altispinus*. Scale in right foreground marked off in cm and inches.

Fig. 2. Measurements of pedal phalanges of hadrosaurs. (A) Non-ungual phalanx in side view, showing how lengths are measured on either the medial or lateral side of the bone. (B) Distal articular view of a non-ungual phalanx, showing the measurement of distal width. (C, D) Measurements of ungual lengths. (C) Side view of bone. (D) Dorsal view of bone, with lines showing medial and lateral length measurements.

Fig. 3. Pedal proportions of hadrosaurs and other bipedal, facultatively bipedal, or potentially bipedal ornithischians. Symbol color key for this and Fig. 4): black and open symbols = basal ornithopods and basal iguanodontians; red = non-hadrosaurian ankylopollexian iguanodontians; green = hadrosaurids; yellow = basal ceratopsians and neoceratopsians. (A) Scatterplot of principal component (PC) 2 against PC 1 of a principal components analysis (Table 2). PC 1 is mostly associated with specimen size. Parameters with

positive loadings on PC 2 are lengths of phalanges distal to the first phalanx of digits II-IV, while parameters with negative loadings on PC2 are lengths of the first phalanx of digits II-IV, and phalanx widths. (B) Scatterplot of an aspect of PC 2 (ratio of the combined lengths of the three distal phalanges of digit III to the length of the first phalanx of digit III) against digit III length. (C) Scatterplot of another aspect of PC 2 (relative width of phalanx III2) against digit III length. (D) Scatterplot of PC 3 against PC 1. Parameters with positive loadings on PC 3 are lengths of the non-ungual phalanges, while parameters with negative loadings on PC 3 are ungual lengths and, to a lesser extent, phalanx widths. (E) Scatterplot of an aspect of PC 3 (ratio of ungual length to the combined lengths of the non-ungual phalanges) of digit III against the length of digit III.

Fig. 4. Relative lengths of digits II, III, and IV of hadrosaurs and other bipedal, facultatively bipedal, or potentially bipedal ornithischians. (A) Scatterplot of the length of digit II relative to the length of digit III, as a function of digit III length. (B) Scatterplot of the length of digit IV relative to the length of digit III, as a function of digit III length. (C) Scatterplot of the length of digit IV relative to the length of digit III, as a function of digit III length.

Fig. 5. Small (TMP 77.17.06) and large (TMP 76.11.11) footprints, *Amblydactylus kortmeyeri* (Currie and Sarjeant 1979), plausibly attributed to the same iguanodontian species, from the Lower Cretaceous Gething Formation of British Columbia. Scale marked in 1-cm increments.

459

460 **Supplemental animation.** Pedal skeletons of juvenile hadrosaurids. (Left) YPM VPPU 22400,
461 composite right foot of *Maiasaura peeblesorum*. (Right) TMP 2016.37.1, left foot of
462 *Prosaurolophus maximus*.

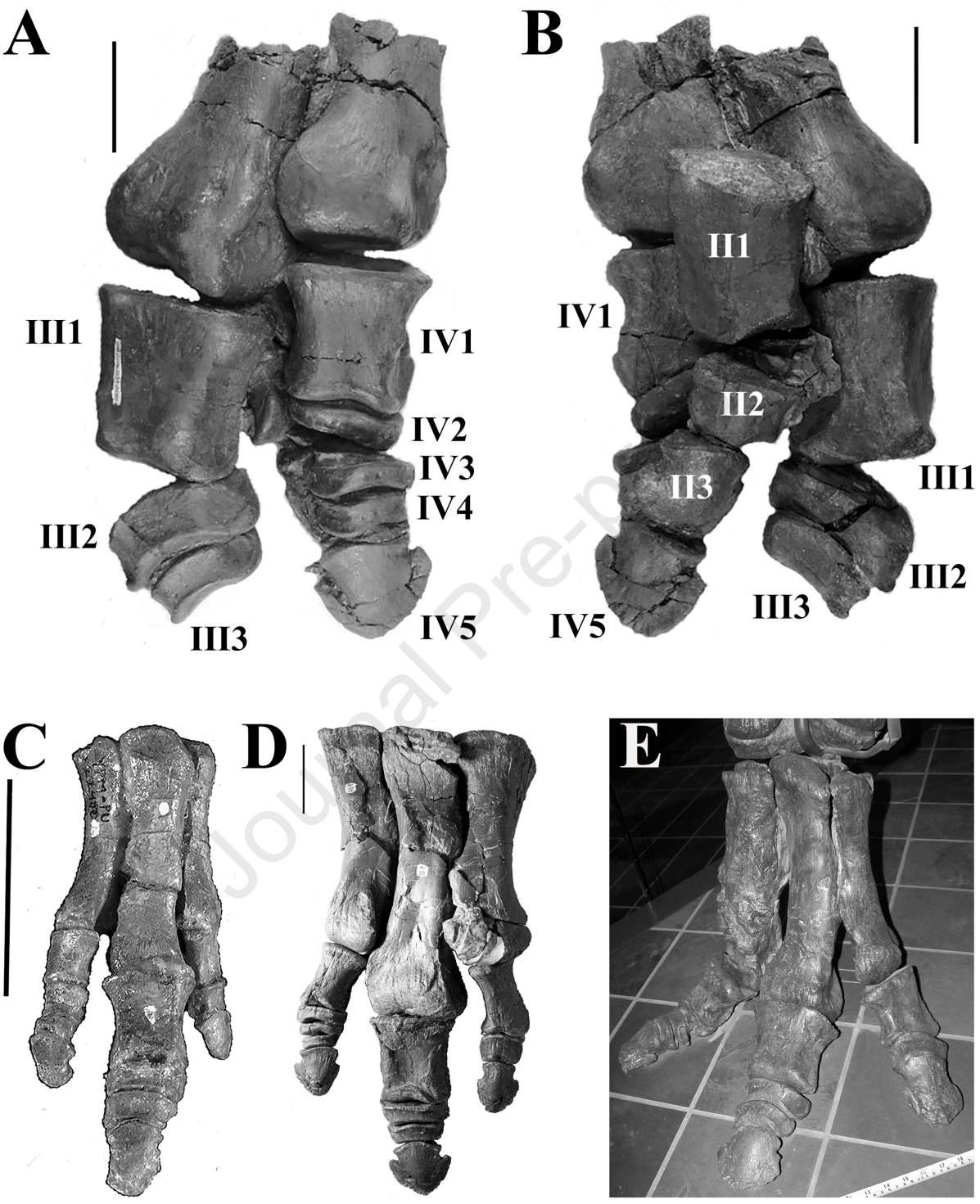

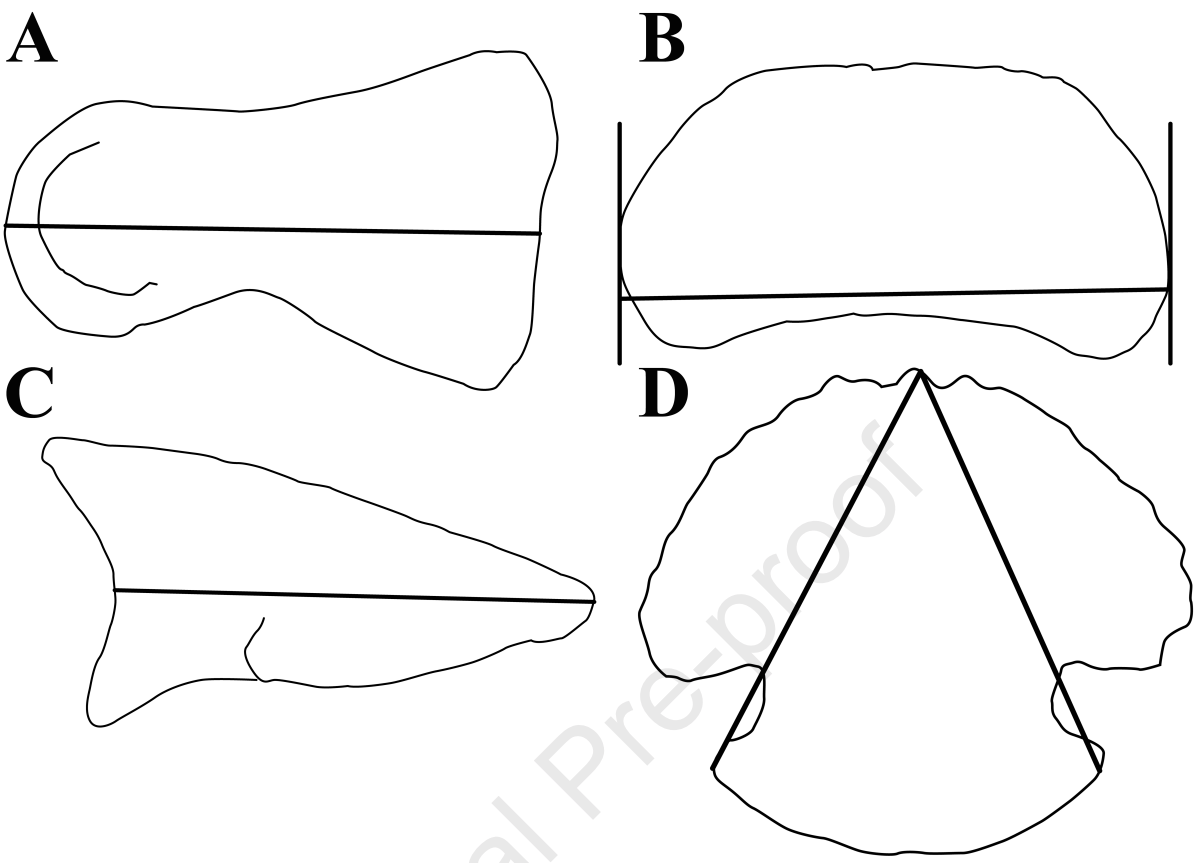

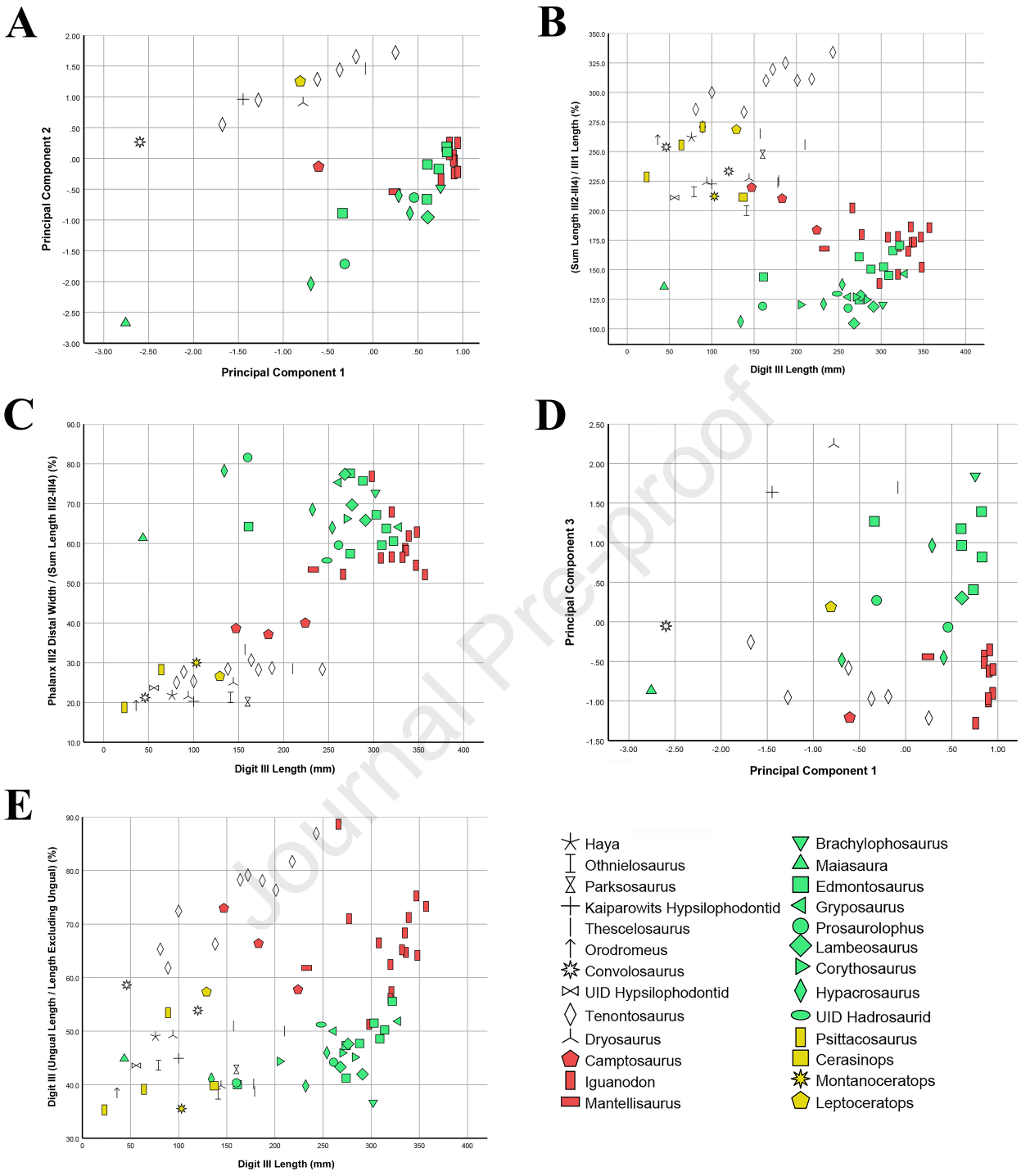

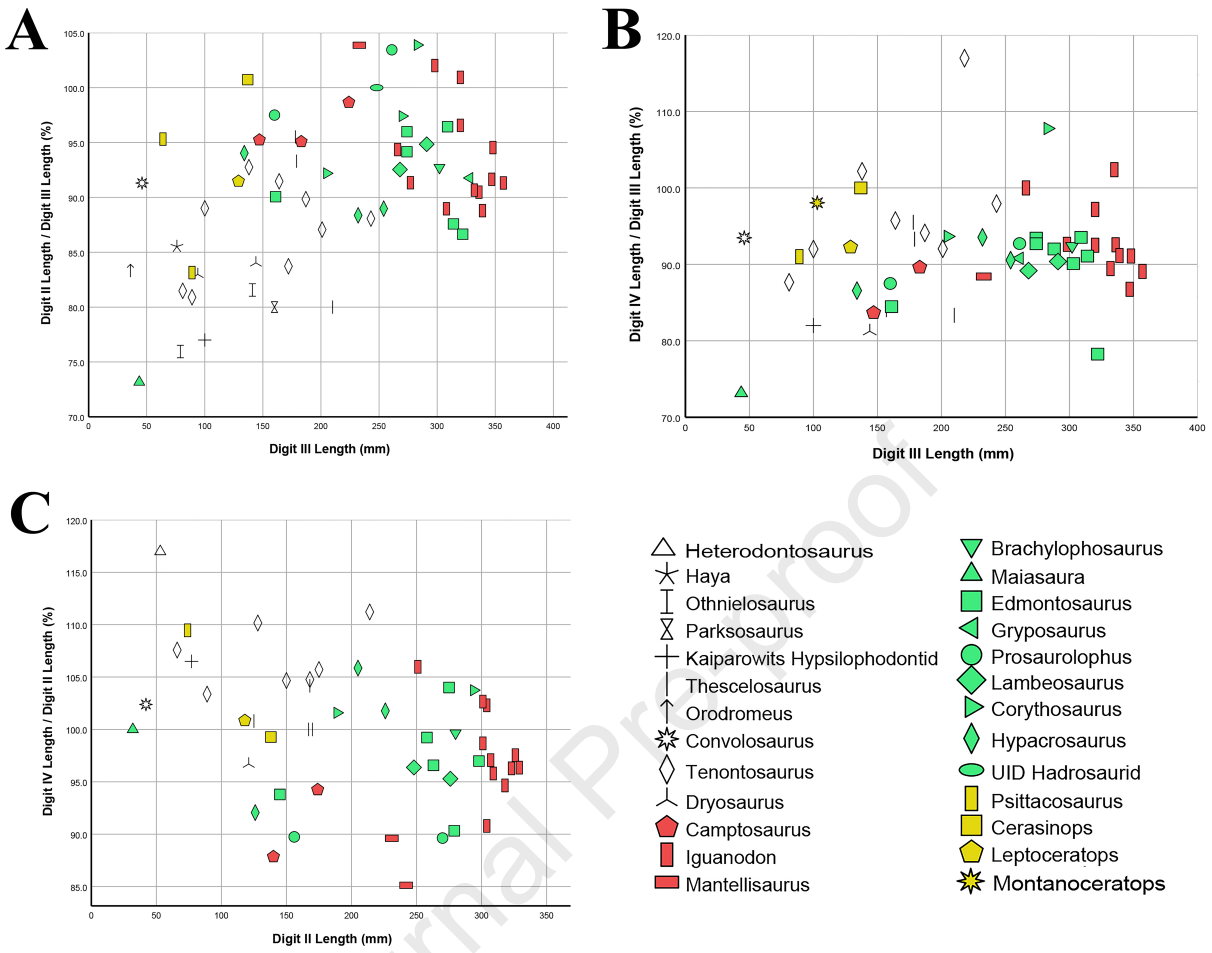

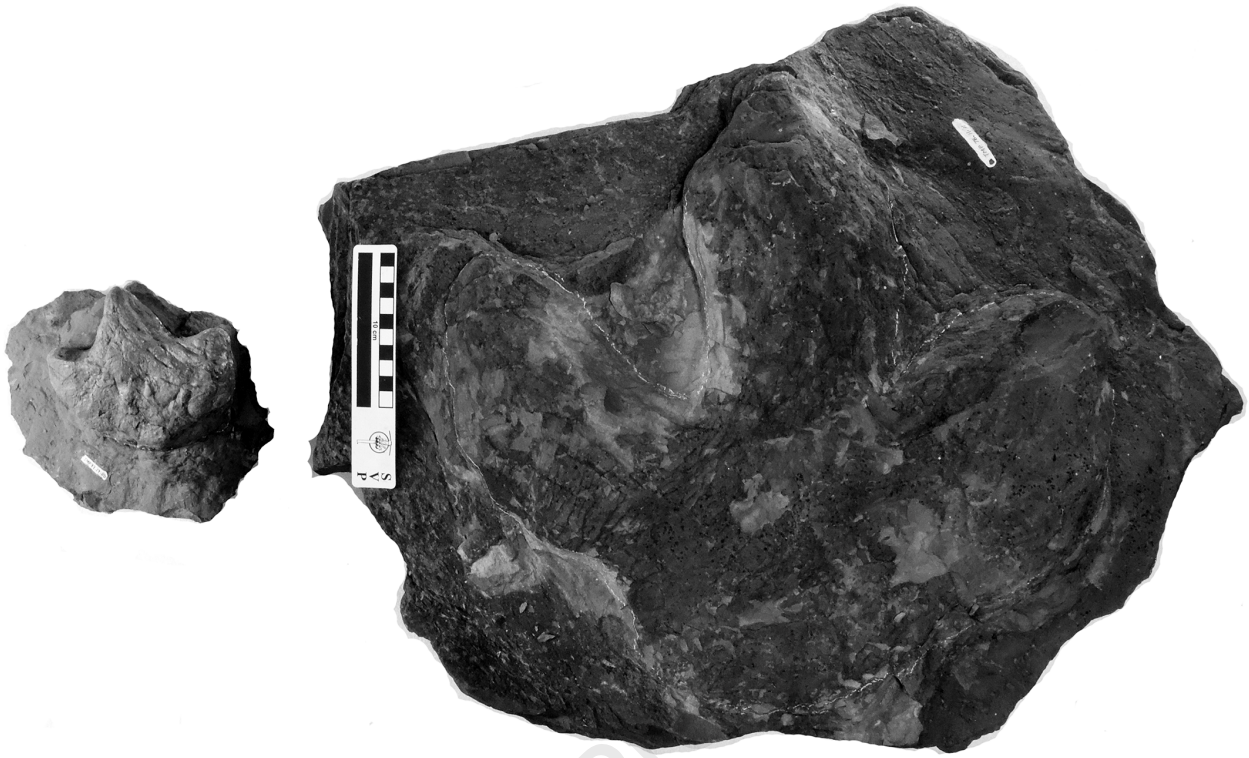

The authors have no conflicts of interest associated with this study.